The Structure of Deprotonated Tri-Alanine and Its a_3^- Fragment Anion by IR Spectroscopy

Jos Oomens[a,b] and Jeffrey D. Steill[a]

[a] FOM Institute for Plasma Physics Rijnhuizen, Nieuwegein, The Netherlands
[b] van't Hoff Institute for Molecular Sciences, University of Amsterdam, Amsterdam, The Netherlands

We present the first infrared spectra of a mass-selected deprotonated peptide anion (AlaAlaAla) and its decarboxylated fragment anion formed by collision induced dissociation. Spectra are obtained by IRMPD spectroscopy using an FTICR mass spectrometer in combination with the free electron laser FELIX. Spectra have been recorded over the 800–1800 cm^{-1} spectral range and compared with density functional theory calculated spectra at the B3LYP/6-31++G(d,p) level for different isomeric structures. These experiments suggest a carboxylate anion for $[M - H]^-$ and an amide deprotonated (amidate) structure for the a_3 fragment anion $[M - H - CO_2]^-$. The frequency for the amidate carbonyl stretch occurring around 1555 ± 5 cm^{-1} has been confirmed by additional spectroscopic studies of the conjugated base of N-methylacetamide, which serves as a simple model system for the deprotonated amide linkage in a peptide anion. (J Am Soc Mass Spectrom 2010, 21, 698–706) © 2010 Published by Elsevier Inc. on behalf of American Society for Mass Spectrometry

While peptide sequencing by collision induced dissociation tandem mass spectrometry (CID MS) has found wide application in biochemistry, the underlying reaction chemistry remains an issue of lively debate. In recent years, the application of infrared (IR) spectroscopy to CID fragment ions has provided important new information on the molecular structures of CID fragment ions, for which several isomeric forms have been suggested. Free electron laser based IR multiple photon dissociation (IRMPD) spectroscopy applied to CID ions generated in a tandem mass spectrometer has been the most influential method in this respect.

The first CID fragment ion IR spectrum was reported by Polfer et al., who showed unambiguously that the b_4 fragment of the Leucine-enkephalin peptide possesses an oxazolone structure [1], as originally suggested by Harrison and coworkers [2]. An important structural question is whether cyclization of the peptide chain occurs upon CID fragmentation, as this may lead to sequence scrambling and hence to the occurrence of non-sequence ions in MS^n spectra [3, 4]. IR spectroscopy indicated that a fraction of the a_4 ions generated from leucine-enkephalin may indeed adopt cyclic structures [5]. In the case of b_2 ions, cyclization would lead to a diketopiperazine structure, which is indeed lower in energy than the isomeric oxazolone b_2 structure. IR spectroscopy showed, however, that b_2 ions generated from protonated AAA [6] and AGG [7] adopt exclusively oxazolone structures, as already predicted on the basis of computations by Paizs and Suhai [8]. Perhaps more surprisingly, the b_2 ions from the doubly protonated tryptic digest peptides YIGSR, YIYGSFK, and YGGFLR were also found to have an oxazolone structure [9], in contrast to what had been speculated on the basis of a statistical analysis of MS^n spectra [10]. b_2 ions formed from some His-containing peptides were spectroscopically shown to adopt diketopiperazine structures [11]. It was also recently shown by IR spectroscopy that the propensity of forming larger cyclic b fragment ions is considerable, and in some cases it is even the dominant fragment structure [12, 13]. Furthermore, IR spectroscopy has among others been applied to elucidate the structure of c-type fragments obtained in electron capture dissociation (ECD) [14] and to show that amide protons may be mobilized in cases where the added proton is strongly sequestered [15].

Peptide sequencing via tandem MS in negative ion mode (i.e., on the deprotonated peptide) is not nearly as popular as its positive ion mode counterpart. This is perhaps somewhat surprising since most instruments can run in both modes (though not necessarily as efficiently [16]) and moreover, additional information from the deprotonated peptide could obviously increase the sequence coverage. For instance, c-type ions are commonly observed in CID of peptide anions [17]. However, the dissociation modes of deprotonated peptides appear to be more complex and are often reported to be more residue-specific, see, e.g., [18–22].

Here we present the first IR spectroscopic investigation of a peptide anion, deprotonated tri-alanine, and of one of its main CID fragments. Peptides without acidic residues are generally assumed to be deprotonated on the C-terminal free acid group [20]. However, other

Address reprint requests to Dr. J. Oomens, FOM Institute for Plasma Physics Rijnhuizen, Edisonbaan 14, Nieuwegein 3439MN, The Netherlands. E-mail: joso@rijnhuizen.nl

1044-0305/10/$32.00
doi:10.1016/j.jasms.2010.01.004

Published online January 22, 2010
Received November 15, 2009
Revised January 4, 2010
Accepted January 4, 2010

deprotonated structures are feasible and may be relatively stable. Condensed-phase computational studies predict amidate structures (also referred to as azaenolates) for the lithium salts of model peptides [23]. Harrison noted that the ESI-generated methyl ester of tri-alanine was deprotonated as efficiently as the free acid tri-alanine [17]. In general, we note that for even simpler systems, isolated amino acids, the question of the deprotonation site has recently been under debate [24], and that IRMPD spectra have proven very helpful in resolving the anion structures [25]. In addition, the lowest energy structures in solution and in the gas phase (i.e., in the mass spectrometer) are not necessarily the same, as aqueous solutions tend to stabilize charge-localized structures by hydrogen bonding; removal of the solvent tends to enhance the relative stability of charge-delocalized structures [26]. Hence, structures exhibiting resonance stabilization by conjugation are of particular interest in gas-phase studies. A remarkable example of this effect has recently been studied with IRMPD spectroscopy for the conjugate base of *para*-hydroxybenzoic acid [27].

For the deprotonated peptides studied here, tautomeric enolate and amidate structures (Scheme **1**) are therefore of particular interest apart from a carboxylate structure. The amidate tautomer is formed by deprotonation on the amide nitrogen atom, while the enolate tautomer is formed by deprotonation of the α-carbon atom.

A common fragmentation channel in the CID of deprotonated peptides is decarboxylation, i.e., the loss of a neutral CO_2 unit from the C-terminus [17]. In peptide fragmentation terminology, this reaction produces the a_n sequence ion from an n-residue peptide. In the absence of acidic residues, an important question is where the charge is localized in this a_n-fragment, which no longer has a carboxylate moiety. Amidate and enolate structures appear to be attractive possibilities, which may gain gas-phase stability from partial charge delocalization, but other structures have actually been suggested for the a_2 fragment of the deprotonated GlyGly anion [28]. In this contribution, we will attempt to determine the structures of deprotonated AAA and its a_3 fragment anion by IRMPD spectroscopy in combination with density functional theory (DFT) calculations.

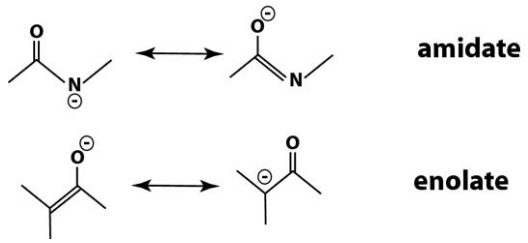

Scheme 1. Resonance structures for amidate (deprotonated amide) and enolate (deprotonated α-carbon) peptide anion tautomers. Note that the amidate motif has also been referred to as 'azaenolate'.

Experimental and Computational Methods

Deprotonated peptide anions were generated by electrospray ionization (Micromass Z-Spray source) in negative ion mode using an ~1 mM solution of tri-alanine (Sigma-Aldrich, Zwijndrecht, The Netherlands) in a $MeOH/H_2O$ mixture, with a few drops of a 1 M solution of NaOH added to aid in the deprotonation of the peptide. The conjugate base of N-methylacetamide gave only a low ion count so that a solution containing 2 mM the sample and 10 mM NaOH was used. The anions are accumulated in a linear hexapole trap before being injected into a home-built Fourier transform ion cyclotron resonance (FTICR) mass spectrometer [29–31] equipped with a 4.7 T actively-shielded superconducting magnet (Cryomagnetics Inc., Oak Ridge, TN, USA). Raising the potential difference between the extraction cone and the DC bias of the first hexapole ion guide results in the formation of CID peptide fragment anions, of which the a_3 anion is one of the more abundant ones, depending on the exact setting of the cone voltage.

In the ICR cell, the anion under study is mass-isolated by a SWIFT excitation pulse [32]. Subsequently, the ions are irradiated with the focused output of the free electron laser FELIX [33]. FELIX produces 5 μs long pulses with an energy of ~60 mJ (30 mJ in the ICR cell) and a bandwidth of ~0.5% of the central wavelength. In these experiments, the wavelength of FELIX is scanned between 5.5 and 13 μm, corresponding to a spectral range of roughly 750–1800 cm^{-1}. Ions are irradiated from 3 to 5 s and a standard excite/detect sequence subsequently detects the extent of fragmentation. At each wavelength point, three mass spectra are averaged and the dissociation yield is determined as the sum of all dissociation products divided by the sum of fragment and parent ions. In the case of deprotonated N-methylacetamide (m/z 72), only very low dissociation into m/z 56 (presumably corresponding to loss of CH_4) was observed and the action spectrum was recorded by monitoring the electron detachment yield instead using a method described previously [34]. In all cases, plotting the yield as function of the photon energy in cm^{-1} was used to produce the IRMPD spectrum.

Optimized anion structures and computed spectra were generated by density functional theory using the B3LYP functional and the 6-31++G(d,p) basis set as implemented in Gaussian 03 rev. C.02. This method was previously found to yield accurate energies for deprotonated systems [35, 36] as well as a good prediction of the infrared spectra of gas-phase carboxylate anions [37]. As the aim of this paper was to determine the isomeric structures, and not a detailed analysis of the conformeric space, a full conformational search of the potential energy surface has not been performed here. Instead, starting structures were produced by 'chemical intuition', where maximizing the number of H-bonding interactions was used as the main guideline. Also, only *trans* configurations of the amide bonds have been consid-

ered [38]. Computed harmonic frequencies are scaled by 0.975 and convoluted with a 20-cm^{-1} FWHM Gaussian lineshape function to facilitate easy comparison with experimental spectra.

Results and Discussion

[AAA − H]$^-$

Three main isomeric motifs have been considered for the deprotonated AAA anion: carboxylate, amidate, and enolate structures. Within these families, many different conformers exist, though we will only discuss those having distinctive H-bonding networks. Optimizing the number of H-bonding interactions leads to two main conformeric motifs within each of the isomeric families: (1) folded structures where the N- and C-termini interact, leaving some of the amide carbonyl and/or NH groups without H-bonding interactions; and (2) quasi-linear conformers where the termini interact with the adjacent amide groups, which also interact with each other. Figure 1 displays low-energy structures for carboxylate and amidate isomers; computed energies for all three isomeric motifs are listed in Table 1. The lowest energy structure found is a carboxylate isomer (**III**), but the energy gap to the lowest amidate structure (**VI**) is relatively small, about 20 kJ/mol. In addition, the quasi-linear conformers appear to be somewhat lower in energy than the folded structures, similar to what was found for positively charged analogs, protonated tri-glycine, although there, the margin was even much smaller [39–41]. The enolate structures are more than 150 kJ/mol higher in energy, in qualitative agreement with computations by Bowie and coworkers, who considered enolate structures as intermediates on the *b/y* fragmentation pathway of deprotonated di-glycine [18].

Table 1. Computed relative ZPE-corrected and free energies (in kJ/mol) for various conformations of carboxylate and amidate isomers of [AAA – H]$^-$ using the B3LYP/6-31++G(d,p) method

#	Type	Fold/linear	ZPE corr energy	Free energy
I	Carboxylate	Folded	+89	+93
II	Amidate	Folded	+77	+75
III	Carboxylate	Linear	0	0
IV	Carboxylate	Folded	+14	+16
VI	Amidate	Linear	+20	+21
VII	Carboxylate	Folded	+9	+13
VIII	Enolate	Linear	+155	+153
IX	Enolate	Folded	+162	+162

Upon IR activation, deprotonated tri-alanine (*m/z* 230) was found to undergo dissociation forming mainly the *m/z* 88 fragment ion. This ion likely corresponds to the y_1 fragment having a deprotonated alanine structure, which is a commonly observed CID product ion for peptides containing only alkyl side chains [17]. Smaller fragment yields are observed at *m/z* 115 (5% of the total IRMPD fragment yield) and *m/z* 87 (3%). Notably, the a_3^- ion at *m/z* 186, subject of the discussion below, is not an IRMPD fragment under our experimental conditions. Figure S1 in the Supporting Information, which can be found in the electronic version of this article, shows a mass spectrum recorded with the FEL at the strong resonance near 1670 cm^{-1}. The IRMPD yield in the 87, 88, and 115 channels is summed giving the spectrum shown in Figure 2. The highest frequency

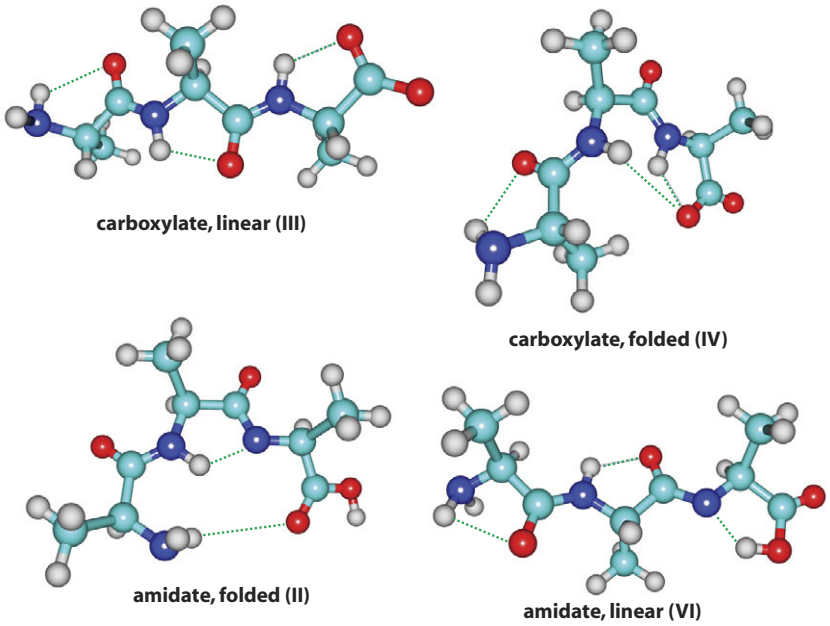

Figure 1. Representative structures for the deprotonated tri-alanine anion in two of its isomeric motifs, carboxylate and amidate, each in two conformeric motifs (linear and folded). Dashed green lines represent H-bonding interactions. Respective energies are given in Table 1.

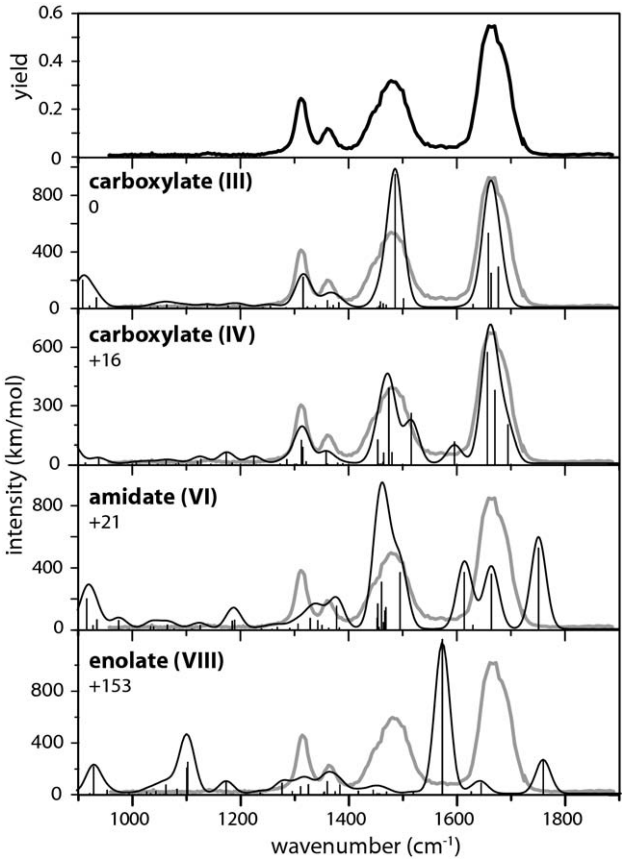

Figure 2. Experimental IRMPD spectrum of $[AAA - H]^-$ (top panel) compared with calculated spectra for low-energy carboxylate, amidate, and enolate structures. Relative free energies in kJ/mol are indicated.

band observed falls well below 1700 cm^{-1}, which makes it unlikely that the species features a COOH moiety, since one would expect to observe a carboxylic acid C = O stretch higher than 1700 cm^{-1} in that case. Hence, amidate and enolate structures appear unlikely based on this simple observation. On the other hand, the spectrum is also not typically that observed for free gas-phase carboxylate species, such as observed by IRMPD spectroscopy for the benzoate anion [37] and several deprotonated amino acids [25]. These spectra are dominated by the symmetric and antisymmetric OCO stretching modes around 1300 and 1600 cm^{-1}, respectively. In fact, the spectrum shown in Figure 2 is more typical for (cationized) peptides, in which the strongest bands result from the collective amide CO stretching and NH bending modes, commonly referred to as amide I and II modes, respectively (see e.g., [5, 40, 42, 43].

Figure 2 compares the experimental spectrum with computed spectra for different candidate structures. It is observed immediately that the computed spectra for the amidate and enolate structures fail to match the experimental spectrum, as expected, based on the qualitative analysis above. The spectrum calculated for the amidate structure shows a strong carboxylic acid C = O stretch at 1760 cm^{-1}, which is clearly not observed experimentally. It is further of interest to note that amidate Structure **VI** is virtually identical to carboxylate Structure **III**, except for the transfer of the proton. Nonetheless, the computed spectra for the two isomers are widely different. Mainly, the carbonyl C = O stretch mode of the deprotonated amide group in the amidate structure is red-shifted due to reduced electron density in the CO bond as a consequence of the conjugation shown in Scheme **1**. In addition, the amide II band around 1500 cm^{-1} is strongly enhanced, which appears to be a consequence of a convolution over several medium-intensity vibrations involving mainly bending modes of the COOH proton, which is strongly hydrogen bonded to the deprotonated amide group. While possibly amidate and enolate structures with lower energy exist, the strong disagreement observed here makes it unlikely that any of those would possess a spectrum matching the experimental one, and we discard the possibility of amidate and enolate structures.

The computed spectra for several carboxylate structures, however, show reasonably good agreement with the experimental IRMPD spectrum. Various conformers of this isomer, constituting structures with different H-bonding networks, have been investigated. Although relative energies for the different H-bonded structures fall within a fairly large range, ~100 kJ/mol, their calculated spectra are very similar. The strongest band in the calculated spectra near 1675 cm^{-1} is a convolution of the two amide carbonyl stretch modes and the carboxylate asymmetric stretch mode. The feature centered around 1500 cm^{-1}, which varies somewhat in shape for the different conformers, is mainly due to the two amide NH bending modes. The weak band consistently observed near 1375 cm^{-1} is due to an umbrella motion of the methyl groups. Finally, the band at 1320 cm^{-1} is due to the symmetric carboxylate stretching mode.

The similarity of the computed spectra for the different carboxylate conformers makes it difficult to assign one of the structures as the conformer present in the experiment. None of the carboxylate structures can truly be eliminated based on the IR spectrum, and multiple low-energy carboxylate conformers may contribute to the observed spectrum, as perhaps suggested by the somewhat broadened feature around 1480 cm^{-1}.

$[AAA - H - CO_2]^-$

The a_3 fragment anion of deprotonated AAA at *m/z* 186 is generated by in-source CID, changing the settings of the cone voltage and the hexapole accumulation trap, and subsequent mass isolation of this species in the ICR cell. IRMPD of this ion results mainly in the formation of a fragment at *m/z* 115, which likely corresponds to the a_2 anion and which is used to record the spectrum of the a_3 anion. The experimental spectrum of a_3^- of deprotonated tri-alanine is significantly different from its intact precursor anion, as is shown in Figure 3. While the

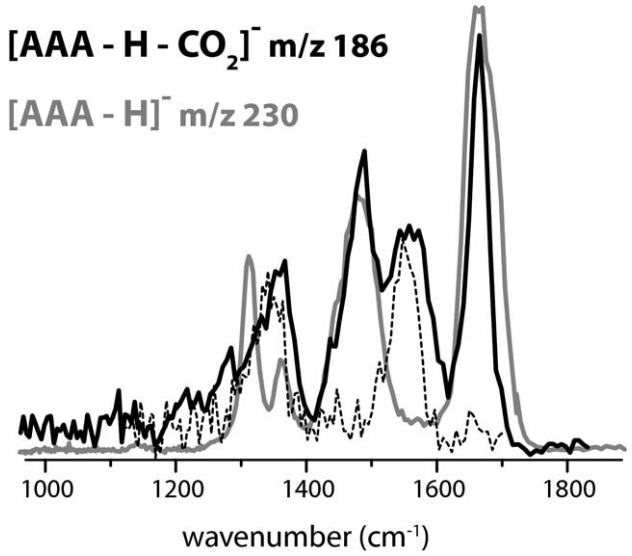

Figure 3. Comparison of the experimental IRMPD spectrum of deprotonated tri-alanine (gray) with that of its a_3 fragment anion (black). The dashed line represents the IRMPD spectrum of the conjugate base of N-methylacetamide.

amide I and amide II bands are still present, a new feature centered around 1560 cm^{-1} appears between them. The amide I band appears to be somewhat narrower and less intense, which is likely due to the absence of a carboxylate antisymmetric stretching mode in the fragment ion. In addition, the 1200–1400 cm^{-1} spectral range, which includes the symmetric OCO stretching mode in the precursor anion $[M - H]^-$, exhibits substantially different features in the fragment anion as a consequence of the absence of the carboxylate moiety.

The main issue in the determination of the structure of the a_3 fragment anion is the location of the formal charge site. As the species no longer has a carboxylate group and the peptide possesses only alkyl residues, there is no 'natural' site for the negative charge to reside. Studies reporting mechanistic details of peptide anion fragmentation often display *a*-ion structures where the charge is located on the α-carbon of the C-terminal residue, see e.g., [17, 28]. For the a_2^- ion of $[GlyGly - H]^-$, it was suggested that a structure with the charge located on the N-terminus is lower in energy [28]. Finally, amidate and enolate ions form interesting candidate structures, which may benefit from resonance stabilization. While enolate anions have been suggested as intermediate structures in peptide anion fragmentation pathways [18], we are not aware of studies suggesting any of these charge-delocalized structures as *a*-type anions.

Since little mechanistic or structural information is available on the formation of the anionic *a*-fragment, optimized structures and computed spectra were generated for a variety of isomeric motifs as displayed in Scheme 2. Note that for each of these motifs, multiple isomers exist and, moreover, multiple conformers exist.

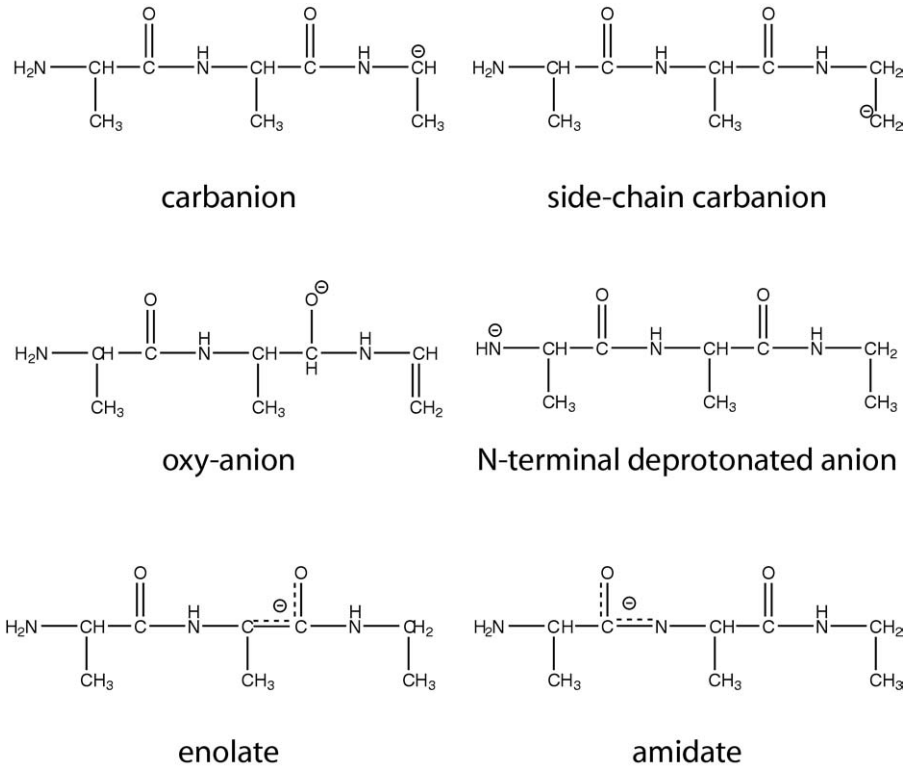

Scheme 2. Classification of isomeric motifs for the $\mathbf{a_3}$ anion from deprotonated tri-alanine considered in this work.

Table 2. Computed relative ZPE-corrected and free energies (in kJ/mol) for selected isomers of $[AAA - H - CO_2]^-$ using the B3LYP/6-31++G(d,p) method. The superscript number refers to the residue (counting from the N-terminus)

#	Motif	ZPE corr energy	Free energy
2	Carbanion	+207	+207
8	sc^1 Carbanion	+195	+198
3	sc^3 Carbanion	+192	+189
10	Oxy-anion	+156	+157
15	$Enolate^2$	+86	+86
16	$Enolate^1$	+81	+78
4	$Amidate^2$	+18	+18
7	$Amidate^2$	+14	+13
13	$Amidate^2$	+8	+8
11	$Amidate^1$	+4	+3
12	$Amidate^1$	0	0

Cartesian coordinates for all structures are given in the Supporting Information.

Table 2 lists some of the structures found with their relative free energies.

Carbanion structures are formed by deprotonation of one of the side-chain methyl groups or of the α-carbon of the third residue, where the cleavage occurred. One notices immediately in Table 2 that these carbanion isomers are typically around 200 kJ/mol higher in energy than the lowest energy structure found. Deprotonation of the C_α-position of the first or second residue leads to enolate structures, where the charge is delocalized over the C_α-atom and the adjacent amide carbonyl (see Scheme **2**). This resonance stabilization brings the relative energies of enolate structures to within ~80 kJ/mol of the lowest energy structure. Placing the charge on the carbonyl oxygen atom without allowing for charge delocalization, such as in the oxy-anion structure (Scheme **2**), increases the relative energy substantially. Amidate anion structures are consistently calculated to have the lowest energies and different conformers typically lie within 20 kJ/mol of each other. Finally, in our calculations, the N-terminal deprotonated isomer, as proposed for the a_2^- ion from deprotonated GlyGly [28], collapsed to an amidate structure with the first amide linkage being deprotonated.

Amidate and enolate isomers are thus the most promising candidate structures. The energy gap of about 80 kJ/mol between enolate and amidate structures is in the range of the energy difference between amidate and enolate tautomers of the conjugate base of N-methylacetamide (see Table 3). Moreover, experimental and computational studies find the amidate tautomer of acetamide to be more stable than the enolate tautomer by ~50 to 80 kJ/mol [23, 36]. The increased stability of the amidate tautomer can be explained by the larger degree of charge delocalization in this tautomer compared with the enolate tautomer, which is illustrated by a comparison of bond lengths in Table 3 and in Figure S2 in the Supporting Information. Compared with neutral N-methylacetamide, the CC bond in the enolate tautomer of its conjugated base strongly contracts (−0.125 Å), indicating the tendency to form a CC double-bond, which localizes the charge largely on the O-atom. For the amidate tautomer on the other hand, the CN and CO bonds contract and expand about equally (−0.043 Å and +0.046 Å, respectively), indicating that the charge is more equally shared between the O and N-atoms, thus truly forming two 2-center-3-electron bonds. Note also that an analysis of the computed vibrations indicates that the carbonyl stretch in the amidate structure is really an asymmetric NCO stretch, i.e., simultaneously involving the NC and CO bonds.

Figure 4 compares the experimental IRMPD spectrum of the a_3 anion with calculated spectra for selected isomers from Table 2. Although the relative intensity of the amide I mode near 1665 cm^{-1} is underestimated in all computed spectra, the positions of the amide I and II bands are reproduced reasonably well by all but the enolate structures. The band around 1560 cm^{-1} that appears only in the fragment and not in the precursor ion (Figure 3) appears as a good diagnostic for the a_3^- structure. Only the amidate and enolate structures reproduce this band, which is due to the amide carbonyl stretching of the deprotonated residue, reflecting the formal reduction in the CO bond order from 2 to 3/2 in these structures. The relative intensity of this band in the enolate tautomer is much larger than that of the other modes, which moreover do not match the experimental band positions particularly well. The computed spectra for the amidate structures, on the other hand, present a reasonable match to the observed amide bands. Moreover, the calculated spectra for amidate structures present a good match in the 1200–1400 cm^{-1} range, where three bands are observed. The calculations reveal that these bands are in fact formed by convolution of a large number of relatively weak modes. The amidate calculations identify the most intense of the three features, centered around 1360 cm^{-1}, as mainly having

Table 3. Computed relative energies of the amidate and enolate tautomers of deprotonated N-methylacetamide (in kJ/mol at the B3LYP/6-31++G(d,p) level) and selected bond lengths in Å; changes relative to neutral N-methylacetamide are given in % in parentheses

Tautomer	Free energy	N–C	C–C	C–O
Neutral		1.367	1.520	1.229
Amidate	0	1.324 (–3.1%)	1.538 (+1.2%)	1.275 (+3.7%)
Enolate	+70	1.462 (+6.9%)	1.395 (–8.2%)	1.268 (+3.2%)

See also Figure S2 in the Supporting Information.

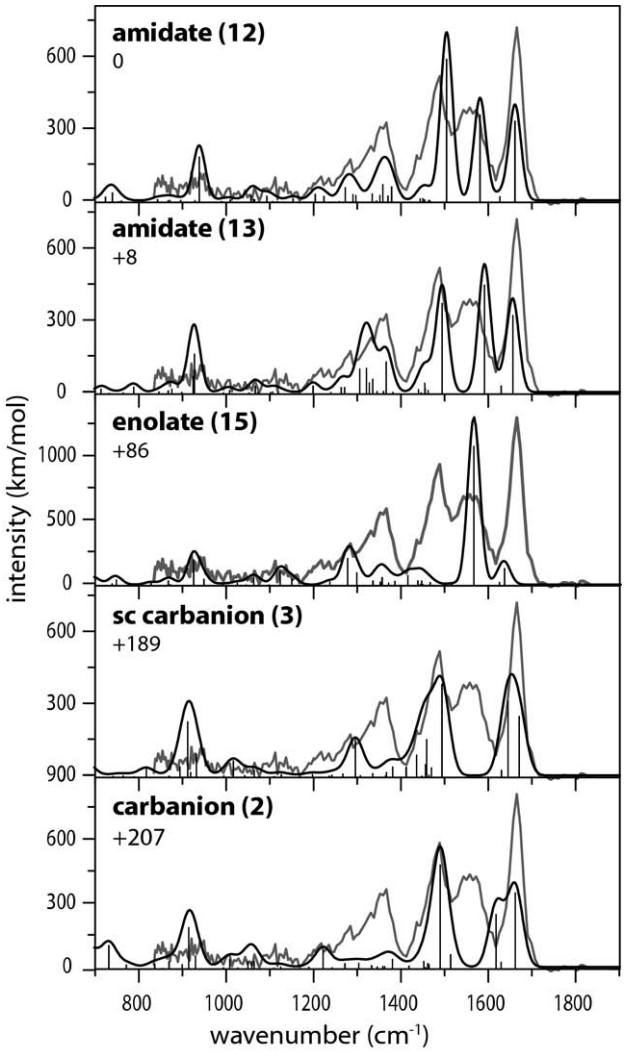

Figure 4. Experimental IRMPD spectrum of the a_3^- fragment ion from deprotonated tri-alanine (gray in all panels) compared with computed spectra for different isomeric structures (black). Relative free energies in kJ/mol are indicated.

NCO scissor character mixed with terminal NH_2 wagging, thus being diagnostic for the amidate structure.

Note that for the a_3^- ion, two amidate isomers exist depending on which of the two amide linkages is deprotonated; structures with the first amide linkage deprotonated are typically slightly lower in energy (about 10 kJ/mol, see Table 2). Of the two amidate isomers, the one with the first amide linkage deprotonated arguably gives a better match with the experimental spectrum (compare **12** and **13** in Figure 4). This slight discrepancy between the two amidate isomers is consistent for different conformers within each isomeric amidate motif, as illustrated in Figure 5. Conformers **11** and **12** are deprotonated on the first amide group, while Conformers **4**, **7**, and **13** are deprotonated on the second amide linkage. For Structures **11** and **12** the amidate carbonyl stretch is slightly (10 cm^{-1}) red-shifted compared to that of **4**, **7**, and **13** (see red and blue lines in Figure 5), bringing it in closer agreement with the experimental spectrum. Moreover, the spectral shape of the three features in the 1200–1400 cm^{-1} range is reproduced significantly better than for Structures **4**, **7**, and **13**, and the NH_2 wagging mode near 930 cm^{-1}, which is only weakly observed, matches well with the predicted position for **11** and **12**. Of the structures deprotonated on the second amide linkage, the spectrum calculated for **13** is close to that of **11** and **12**, which is likely due to strong hydrogen bond between the amide NH and the deprotonated amide N-atom making this structure very similar to Structure **12**.

One notices that all calculated spectra predict the most diagnostic band, the CO stretch of the deprotonated amide, slightly blue shifted compared with the experimental position. To further confirm that our assignment is nonetheless correct, we recorded the IRMPD spectrum of the conjugated base of N-methylacetamide, see Figure S3 in the Supporting Information. Comparison of the experimental spectrum with computed spectra shows that the molecule deprotonates on the amide N-atom forming an amidate and not on the methyl forming an enolate. This is in agreement with the computed energy difference of ~80 kJ/mol, as shown in Table 3. Moreover, comparison of the experimental IRMPD spectrum with the computed amidate spectrum shows that the CO stretch band of the deprotonated amide group is predicted to be ~15 cm^{-1} too high when using the B3LYP/6-31++G(d,p) method and a scaling factor of 0.975. Direct comparison of the experimental IRMPD spectra (see Figure 3) indeed shows that the band assigned as the deprotonated amide CO stretch in a_3^- falls at the same position as the corresponding band in deprotonated N-methylacetamide, providing further support for our assignment of the a_3^- structure as an amidate anion.

Comparison of theory and experiment thus strongly suggests that the a_3^- ion has an amidate structure. The isomer with deprotonation on the first amide linkage matches the experimental spectrum slightly better and is, in addition, slightly lower in energy. However, the second amidate isomer cannot be excluded and may well contribute to the population.

Conclusions

We have presented the first gas-phase IR spectra for a deprotonated peptide and one of its CID fragment ions. Comparison with calculated spectra shows convincingly that tri-alanine is deprotonated on the C-terminal free acid group and not on one of the amide groups. For the protonated analogue, as well as for protonated GGG, protonation at the N-terminus is virtually isoenergetic with protonation at one of the amide groups and, hence, both isomers co-exist [39–41]. Deprotonation of AAA, on the other hand, occurs solely at the C-terminus. Hence, the amide group can compete in basicity with the N-terminus, but not in acidity with the

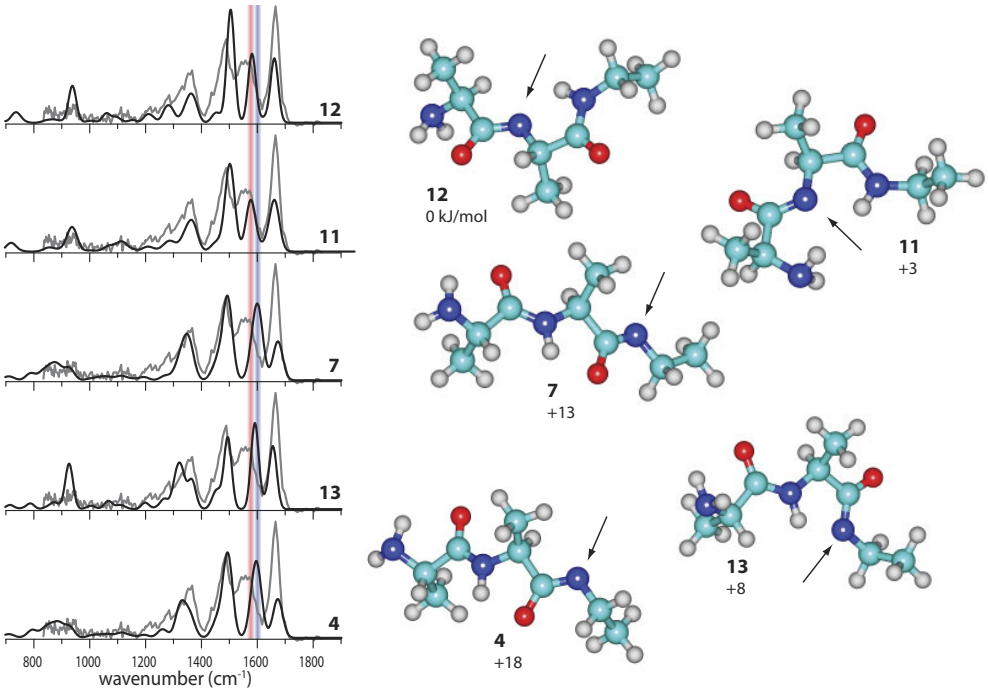

Figure 5. Experimental IRMPD spectrum of $[AAA - H - CO_2]^-$ compared with computed spectra for different conformers of the two amidate isomers. Relative free energies and the site of deprotonation are indicated for each structure. Structures **11** and **12** (**4**, **7**, and **13**) are deprotonated on the first (second) amide linkage. The red (blue) line indicates the approximate position of the deprotonated amide carbonyl stretch in the isomer with deprotonation on the first (second) amide linkage.

C-terminus, despite the resonance structure in the amidate moiety.

The spectrum of the a_3^- fragment generated by CID reveals that this ion is deprotonated on one of the amide groups forming an amidate anion. Amidate structures are consistently lower in energy than enolate structures, likely due to more efficient resonance stabilization in the NCO unit compared with the CCO unit. The energy gap of around 80 kJ/mol between enolate and amidate structures is comparable to that between amidate and enolate tautomers of N-methylacetamide computed at the same level of theory.

In conclusion, this study shows that structural characterization of CID peptide fragments by IRMPD spectroscopy, which has been so successful for protonated peptides, can be applied to deprotonated peptides as well. Knowledge of these fragment structures is expected to eventually enhance our understanding of the fragmentation pathways of peptide anions. Further studies in our laboratory will investigate whether the presently found amidate structure occurs generally for anionic *a*-type fragments and what the influence of non-alkyl side chains is.

Acknowledgments

The authors acknowledge that this work is part of the research program of FOM, which is financially supported by The Nederlandse Organisatie voor Wetenschappelijk Onderzoek (NWO). The authors gratefully acknowledge the expert support by Britta Redlich, Lex van der Meer, and others at the FELIX staff. They acknowledge Richard O'Hair of the University of Melbourne for an insightful discussion on the *a*-anion structure, and Gert von Helden of the Fritz-Haber Institute in Berlin for the loan of the ESI ion source.

Appendix A
Supplementary Material

Supplementary material associated with this article may be found in the online version at doi:10.1016/j.jasms.2010.01.004.

References

1. Polfer, N. C.; Oomens, J.; Suhai, S.; Paizs, B. Spectroscopic and Theoretical Evidence for Oxazolone Ring Formation in Collision-Induced Dissociation of Peptides. *J. Am. Chem. Soc.* **2005,** *127*, 17154–17155.
2. Yalcin, T.; Khouw, C.; Csizmadia, I. G.; Peterson, M. R.; Harrison, A. G. Why Are b Ions Stable Species in Peptide Spectra? *J. Am. Soc. Mass Spectrom.* **1996,** *6*, 1164–1174.
3. Harrison, A. G. Peptide Sequence Scrambling Through Cyclization of b_5 Ions. *J. Am. Soc. Mass Spectrom.* **2008,** *19*, 1776–1780.
4. Bleiholder, C.; Osburn, S.; Williams, T. D.; Suhai, S.; Van Stipdonk, M.; Harrison, A. G.; Paizs, B. Sequence-Scrambling Fragmentation Pathways of Protonated Peptides. *J. Am. Chem. Soc.* **2008,** *130*, 17774–17789.
5. Polfer, N. C.; Oomens, J.; Suhai, S.; Paizs, B. Infrared Spectroscopy and Theoretical Studies on Gas-Phase Protonated Leu-enkephalin and Its Fragments: Direct Experimental Evidence for the Mobile Proton. *J. Am. Chem. Soc.* **2007,** *129*, 5887–5897.
6. Oomens, J.; Young, S.; Molesworth, S.; van Stipdonk, M. Spectroscopic Evidence for an Oxazolone Structure of the b_2 Fragment Ion from Protonated Tri-Alanine. *J. Am. Soc. Mass Spectrom.* **2009,** *20*, 334–339.

7. Yoon, S. H.; Chamot-Rooke, J.; Perkins, B. R.; Hilderbrand, A. E.; Poutsma, J. C.; Wysocki, V. H. IRMPD Spectroscopy Shows That AGG Forms an Oxazolone b_2^+ Ion. *J. Am. Chem. Soc.* **2008,** *130*, 17644–17645.
8. Paizs, B.; Suhai, S. Towards Understanding the Tandem Mass Spectra of Protonated Oligopeptides. 1. Mechanism of Amide Bond Cleavage. *J. Am. Soc. Mass Spectrom.* **2004,** *15*, 103–113.
9. Bythell, B. J.; Erlekam, U.; Paizs, B.; Maitre, P. Infrared Spectroscopy of Fragments from Doubly Protonated Tryptic Peptides. *Chem. Phys. Chem.* **2009,** *10*, 883–885.
10. Savitski, M. M.; Falth, M.; Fung, Y. M. E.; Adams, C. M.; Zubarev, R. A. Bifurcating Fragmentation Behavior of Gas-Phase Tryptic Peptide Dications in Collisional Activation. *J. Am. Soc. Mass Spectrom.* **2008,** *19*, 1755–1763.
11. Perkins, B. R.; Chamot-Rooke, J.; Yoon, S. H.; Gucinski, A. C.; Somogyi, A.; Wysocki, V. H. Evidence of Diketopiperazine and Oxazolone Structures for HA b_2^+ Ion. *J. Am. Chem. Soc.* **2009,** *131*, 17528–17529.
12. Erlekam, U.; Bythell, B. J.; Scuderi, D.; Van Stipdonk, M.; Paizs, B.; Maitre, P. Infrared Spectroscopy of Fragments of Protonated Peptides: Direct Evidence for Macrocyclic Structures of b_5 Ions. *J. Am. Chem. Soc.* **2009,** *131*, 11503–11508.
13. Chen, X.; Yu, L.; Steill, J. D.; Oomens, J.; Polfer, N. C. Effect of Peptide Fragment Size on the Propensity of Cyclization in Collision-Induced Dissociation: Oligoglycine b_2–b_8. *J. Am. Chem. Soc.* **2009,** *131*, 18272–18282.
14. Frison, G.; van der Rest, G.; Turecek, F.; Besson, T.; Lemaire, J.; Maitre, P.; Chamot-Rooke, J. Structure of Electron-Capture Dissociation Fragments from Charge-Tagged Peptides Probed by Tunable Infrared Multiple Photon Dissociation. *J. Am. Chem. Soc.* **2008,** *130*, 14916–14917.
15. Molesworth, S.; Leavitt, C. M.; Groenewold, G. S.; Oomens, J.; Steill, J. D.; Van Stipdonk, M. Spectroscopic Evidence for Mobilization of Amide Position Protons During CID of Model Peptide Ions. *J. Am. Soc. Mass Spectrom.* **2009,** *20*, 1841–1845.
16. Zilch, L. W.; Maze, J. T.; Smith, J. W.; Ewing, G. E.; Jarrold, M. F. Charge Separation in the Aerodynamic Breakup of Micrometer-Sized Water Droplets. *J. Phys. Chem. A* **2008,** *112*, 13352–13363.
17. Harrison, A. G. Sequence-Specific Fragmentation of Deprotonated Peptides Containing H or Alkyl Side Chains. *J. Am. Soc. Mass Spectrom.* **2001,** *12*, 1–13.
18. Bowie, J. H.; Brinkworth, C. S.; Dua, S. Collision-Induced Fragmentations of the $(M - H)^-$ Parent Anions of Underivatized Peptides: An Aid to Structure Determination and Some Unusual Negative Ion Cleavages. *Mass Spectrom. Rev.* **2002,** *21*, 87–107.
19. Brinkworth, C. S.; Dua, S.; McAnoy, A. M.; Bowie, J. H. Negative Ion Fragmentations of Deprotonated Peptides: Backbone Cleavages Directed Through both Asp and Glu. *Rapid Commun. Mass Spectrom.* **2001,** *15*, 1965–1973.
20. Marzluff, E. M.; Campbell, S.; Rodgers, M. T.; Beauchamp, J. L. Low-Energy Dissociation of Small Deprotonated Peptides in the Gas Phase. *J. Am. Chem. Soc.* **1994,** *116*, 7787–7796.
21. Waugh, R. J.; Bowie, J. H. A Review of the Collision Induced Dissociations of Deprotonated Dipeptides and Tripeptides. An Aid to Structure Determination. *Rapid Commun. Mass Spectrom.* **1994,** *8*, 169–173.
22. Harrison, A. G. Effect of Phenylalanine on the Fragmentation of Deprotonated Peptides. *J. Am. Soc. Mass Spectrom.* **2002,** *13*, 1242–1249.
23. Feigel, M.; Martinek, G.; Sauer, W. H. B. What Do Ab Initio Calculations Predict for the Structure of Lithiated Azaenolates of Peptides? *Chem. Eur. J.* **1996,** *2*, 9–18.
24. Tian, Z.; Pawlow, A.; Poutsma, J. C.; Kass, S. R. Are Carboxyl Groups the Most Acidic Sites in Amino Acids? Gas-Phase Acidity, H/D Exchange Experiments, and Computations on Cysteine and Its Conjugate Base. *J. Am. Chem. Soc.* **2007,** *129*, 5403–5407.
25. Oomens, J.; Steill, J. D.; Redlich, B. Gas-Phase IR Spectroscopy of Deprotonated Amino Acids. *J. Am. Chem. Soc.* **2009,** *131*, 4310–4319.
26. McMahon, T. B.; Kebarle, P. Intrinsic Acidities of Substituted Phenols and Benzoic Acids Determined by Gas-Phase Proton Transfer Equilibria. *J. Am. Chem. Soc.* **1977,** *99*, 2222–2230.
27. Steill, J. D.; Oomens, J. Gas-Phase Deprotonation of p-Hydroxybenzoic Acid Investigated by IR Spectroscopy: Solution-Phase Structure Is Retained upon ESI. *J. Am. Chem. Soc.* **2009,** *131*, 13570–13571.
28. Styles, M. L.; O'Hair, R. A. J. The $[M - H - CO_2]^-$ Anion From Glycyl Glycine Undergoes Rearrangement in the Gas Phase. *Rapid Commun. Mass Spectrom.* **1998,** *12*, 809–812.
29. Valle, J. J.; Eyler, J. R.; Oomens, J.; Moore, D. T.; van der Meer, A. F. G.; von Helden, G.; Meijer, G.; Hendrickson, C. L.; Marshall, A. G.; Blakney, G. T. Free Electron Laser-Fourier Transform Ion Cyclotron Resonance Mass Spectrometry Facility for Obtaining Infrared Multiphoton Dissociation Spectra of Gaseous Ions. *Rev. Sci. Instrum.* **2005,** *76*, 023103.
30. Polfer, N. C.; Oomens, J. Reaction Products in Mass Spectrometry Elucidated with Infrared Spectroscopy. *Phys. Chem. Chem. Phys.* **2007,** *9*, 3804–3817.
31. Mize, T. H.; Taban, I.; Duursma, M.; Seynen, M.; Konijnenburg, M.; Vijftigschild, A.; Doornik, C. V.; Rooij, G. V.; Heeren, R. M. A. A Modular Data and Control System to Improve Sensitivity, Selectivity, Speed of Analysis, Ease of Use, and Transient Duration in an External Source FTICR-MS. *Int. J. Mass Spectrom.* **2004,** *235*, 243–253.
32. Marshall, A. G.; Wang, T. C. L.; Ricca, T. L. Tailored Excitation for Fourier Transform Ion Cyclotron Resonance Mass Spectrometry. *J. Am. Chem. Soc.* **1985,** *107*, 7893–7897.
33. Oepts, D.; van der Meer, A. F. G.; van Amersfoort, P. W. The Free-Electron-Laser User Facility FELIX. *Infrared Phys. Technol.* **1995,** *36*, 297–308.
34. Steill, J. D.; Oomens, J. Action Spectroscopy of Gas-Phase Carboxylate Anions by Multiple Photon IR Electron Detachment/Attachment. *J. Phys. Chem. A* **2009,** *113*, 4941–4946.
35. Merrill, G. N.; Kass, S. R. Calculated Gas-Phase Acidities Using Density Functional Theory: Is It Reliable? *J. Phys. Chem.* **1996,** *100*, 17465–17471.
36. Hare, M. C.; Marimanikkuppam, S. S.; Kass, S. R. Acetamide Enolate: Formation, Reactivity, and Proton Affinity. *Int. J. Mass Spectrom.* **2001,** 210/211, 153–163.
37. Oomens, J.; Steill, J. D. Free Carboxylate Stretching Modes. *J. Phys. Chem. A* **2008,** *112*, 3281–3283.
38. Paizs, B.; Suhai, S. Combined Quantum Chemical and RRKM Modeling of the Main Fragmentation Pathways of Protonated GGG. I. Cis-*trans* Isomerization Around Protonated Amide Bonds. *Rapid Commun. Mass Spectrom.* **2001,** *15*, 2307–2323.
39. Rodriguez, C. F.; Cunje, A.; Shoeib, T.; Chu, I. K.; Hopkinson, A. C.; Siu, K. W. M. Proton Migration and Tautomerism in Protonated Triglycine. *J. Am. Chem. Soc.* **2001,** *123*, 3006–3012.
40. Gregoire, G.; Gaigeot, M. P.; Marinica, D. C.; Lemaire, J.; Schermann, J. P.; Resonant Infrared Multiphoton Dissociation Spectroscopy of Gas-Phase Protonated Peptides. Experiments and Car-Parrinello Dynamics at 300 K. *Phys. Chem., Chem. Phys.* **2007,** *9*, 3082–3097.
41. Wu, R.; McMahon, T. B. Infrared Multiple Photon Dissociation Spectroscopy as Structural Confirmation for GlyGlyGlyH+ and AlaAlaAlaH+ in the Gas Phase. Evidence for Amide Oxygen as the Protonation Site. *J. Am. Chem. Soc.* **2007,** *129*, 11312–11313.
42. Prell, J. S.; Demireva, M.; Oomens, J.; Williams, E. R. Role of Sequence in Salt-Bridge Formation for Alkali Metal Cationized GlyArg and ArgGly Investigated with IRMPD Spectroscopy and Theory. *J. Am. Chem. Soc.* **2009,** *131*, 1232–1242.
43. Dunbar, R. C.; Steill, J. D.; Polfer, N. C.; Oomens, J. Gas-Phase Infrared Spectroscopy of the Protonated Dipeptides H^+PheAla and H^+AlaPhe Compared with Condensed-Phase Results. *Int. J. Mass Spectrom.* **2009,** *283*, 77–84.